frontiers in Marine Science

TYPE Original Research
PUBLISHED 04 March 2026
DOI 10.3389/fmars.2026.1716162

OPEN ACCESS

EDITED BY
Irene García-Meilán,
University of Barcelona, Spain

REVIEWED BY
Amit Ranjan,
Tamil Nadu Fisheries University, India
Naveen Ranasinghe,
National Chung Hsing University, Taiwan

*CORRESPONDENCE
Chandrasekar Selvam
fishochand@gmail.com

RECEIVED 30 September 2025
REVISED 14 January 2026
ACCEPTED 28 January 2026
PUBLISHED 04 March 2026

CITATION
A M, Selvam C, Santosh TT, N KJS, Prabu D L, Ebeneezar S, Gora AH, P S, Gop AP, S TC, Pradhan C and Chakraborty K (2026) Salinity-induced modulation of hepatic morphology, enzymatic responses, muscle fatty acid composition, and gene expression in the euryhaline teleost *Oryzias dancena*. *Front. Mar. Sci.* 13:1716162. doi: 10.3389/fmars.2026.1716162

Salinity-induced modulation of hepatic morphology, enzymatic responses, muscle fatty acid composition, and gene expression in the euryhaline teleost *Oryzias dancena*

Mariselvammurugan A[1,2], Chandrasekar Selvam[1]*, Tari Tejas Santosh[1,2], Kamini Jothi Sri N[1], Linga Prabu D[3], Sanal Ebeneezar[1], Adnan H. Gora[1], Sayooj P[1], Ambarish P. Gop[4], Tejpal C. S[5], Chiranjiv Pradhan[2] and Kajal Chakraborty[6]

[1]Marine Biotechnology Fish Nutrition and Health Division, ICAR-Central Marine Fisheries Research Institute, Kochi, Kerala, India, [2]Department of Aquaculture, Kerala University of Fisheries and Ocean Studies, Kochi, Kerala, India, [3]Tuticorin Regional Station of ICAR-Central Marine Fisheries Research Institute, Tuticorin, Tamil Nadu, India, [4]Vizhinjam Regional Centre of ICAR-Central Marine Fisheries Research Institute, Thiruvananthapuram, Kerala, India, [5]Biochemistry & Nutrition Division, IICAR-Central Institute of Fisheries Technology, Kochi, Kerala, India, [6]ICAR-National Bureau of Fish Genetic Resources, Lucknow, India

Salinity strongly influences osmoregulation energy metabolism, and physiological performance in euryhaline fishes. The marine medaka, *Oryzias dancena* is an emerging model for investigating the molecular and physiological basis of salinity adaptation. Here, fish were exposed to hypo- (5 ppt), near-isoosmotic (23 ppt), and hyperosmotic (35 ppt) salinities, and assessed integrated physiological, biochemical, and molecular responses. Hepatic histology showed pronounced vacuolization at 5 and 35 ppt, whereas 23 ppt supported more uniform hepatocellular morphology. Whole-body digestive and antioxidant enzymes exhibited salinity-dependent modulation, with elevated protease and SOD activity at 5 ppt and higher lipase activity at 23 ppt. Gene expression analysis showed upregulation of *nka* under salinity extremes, while lipid oxidation genes (*ppar-δ, cpt1*) peaked at 23 ppt, indicating a trade-off between osmoregulatory demand and lipid catabolism. Muscle fatty acid composition remained largely conserved; however, hyperosmotic stress (35 ppt) caused a significant decline in docosahexaenoic acid (DHA, 22:6n-3), together with a concomitant increase in monounsaturated fatty acids, particularly palmitoleic acid (16:1), indicating selective changes in membrane lipid composition under high salinity. Although hepatic fatty acid composition was not measured in this study, the combined evidence from hepatocellular morphology and lipid metabolic gene expression provides clear indications of salinity-dependent shifts in hepatic lipid handling. Collectively, this study provides foundational insight into the osmoregulatory and metabolic strategies of *O. dancena*, establishing its value as a tractable marine model for integrative studies on salinity adaptation.

KEYWORDS
euryhaline, lipid remodelling, marine model fish, nutrigenomics, *Oryzias dancena*, salinity stress

1 Introduction

Environmental salinity is a major abiotic factor influencing energy metabolism, osmoregulation, and overall physiological performance and health in fish (Bal et al., 2021; Bœuf and Payan, 2001; Evans and Kültz, 2020; Tseng and Hwang, 2008). Euryhaline fishes exhibit remarkable physiological plasticity that allows them to tolerate wide salinity fluctuations through coordinated adjustments in ion transport, water balance, and metabolic fuel allocation. These adaptations involve not only changes in ionregulatory mechanisms but also substantial shifts in lipid metabolism, which provides both structural components for cellular membranes and a key energy source supporting osmoregulatory processes (Evans, 2008; Tseng and Hwang, 2008; Edwards and Marshall, 2012; Ern et al., 2014). Despite considerable progress in understanding ion transport mechanisms, relatively less attention has been given to how salinity fluctuations impact lipid metabolism at both tissue and molecular levels. Salinity driven osmotic gradients force euryhaline fishes to reorganize ion transport, water balance, and energy metabolism in order to maintain cellular homeostasis (Bœuf and Payan, 2001; Kültz, 2015) and this process is energetically demanding. A major component of this cost arises from Na^+/K^+-ATPase (*nka*), a primary ion pump responsible for sustaining electrochemical gradients. Elevation of NKA activity at salinity extremes increases ATP requirements, thereby influencing metabolic pathways, particularly mitochondrial β-oxidation and hepatic lipid mobilization (Evans and Kültz, 2020; Tseng and Hwang, 2008). Because lipids act as dense energy reserves and regulate membrane fluidity, salinity acclimation often triggers adjustments in fatty acid profiles and expression of genes regulating LC-PUFA biosynthesis and lipid oxidation (Bœuf and Payan, 2001; Monroig et al., 2013; Tocher, 2003). Thus, osmoregulatory demand mediated through NKA is intrinsically linked to lipid metabolic pathways such as PPAR-regulated β-oxidation and LC-PUFA biosynthesis, highlighting the importance of an integrative approach when examining salinity-driven metabolic adjustments.

The liver plays a central role in these adjustments, coordinating lipid mobilization and storage to meet energy demands imposed by salinity stress. Exposure to hypo- or hyperosmotic conditions can disrupt hepatic lipid homeostasis, often leading to vacuolization and altered expression of lipid metabolic genes (Evans and Kültz, 2020; Kültz, 2015). While moderate, near-isosmotic salinities typically support optimal nutrient assimilation and metabolic efficiency, extreme conditions elevate metabolic costs, forcing a trade-off between energy allocation for osmoregulation and other physiological functions (Bœuf and Payan, 2001; Imsland et al., 2001). These metabolic shifts are often reflected in tissue-specific fatty acid profiles, that membrane fluidity and function under osmotic challenge. Notably, long-chain polyunsaturated fatty acids (LC-PUFA) like docosahexaenoic acid (DHA) are vital for membrane integrity, and its depletion under stress can induce deficiency (Sargent et al., 2003; Tocher, 2003).

Muscle tissue commonly maintains stricter homeostasis in membrane FA composition than the liver, but selective changes, especially in docosahexaenoic acid (DHA, 22:6n-3), are often observed under osmotic or dietary stress and can affect membrane fluidity and cellular signalling (Sargent et al., 2003; Tocher, 2003; Xie et al., 2021). Studies on the influence of rearing salinity on tissue LC-PUFA levels indicate inconsistent findings. While some report increases in EPA and DHA at higher salinities (Dong et al., 2020; Marrero et al., 2021), others observe a depletion of DHA under osmotic stress (Liu et al., 2017). These divergent patterns highlight that the net fatty acid outcome is governed by a complex interplay of species-specific metabolism, dietary input, and the balance between LC-PUFA biosynthesis and catabolism (Tocher, 2010; Monroig et al., 2013). In addition to lipid remodelling, digestive and antioxidant systems also respond to salinity variation and modulate the organism's capacity to supply metabolic fuel and to counteract stress-induced reactive oxygen species (ROS). Salinity-dependent modulation of digestive enzymes such as proteases and lipases can alter nutrient partitioning and energy supply, as shown in American shad (*Alosa sapidissima*) (Liu et al., 2017), yellowfin tuna (*Thunnus albacares*) (Zhang et al., 2023), and Spotbanded Scat (*Selenotoca multifasciata*) (Liu et al., 2024). Concurrently, the induction of antioxidant defenses, including superoxide dismutase (SOD), catalase, and total antioxidant capacity (TAC), helps to mitigate oxidative stress that arises under osmotic extremes (Atli et al., 2006; Lushchak, 2011; Martínez-Álvarez et al., 2005). This interplay between energy acquisition and oxidative stress management is therefore critical for sustaining energy balance under salinity stress.

The marine medaka (*Oryzias dancena*), also known as the Indian Ricefish, has emerged as a promising model for studying the mechanisms of salinity adaptation due to its remarkable euryhalinity, ranging from freshwater to hypersaline conditions. Its close phylogenetic relation to the well-established model *Oryzias latipes* provides a valuable comparative framework, particularly for osmoregulatory studies (Ranjan et al., 2022). However, a comprehensive understanding of the interactive effects of salinity on lipid metabolic pathways that integrates histological, biochemical, and molecular responses is lacking for this species. In particular, no previous study has jointly examined hepatic histomorphology, enzymatic responses, lipid metabolic gene expression, and tissue fatty acid composition across salinity gradients in *Oryzias dancena*. The present study addresses this gap by providing an integrated physiological characterization of salinity-dependent metabolic adjustments in this emerging euryhaline model. Rather than proposing new osmoregulatory mechanisms, this work establishes foundational baseline data necessary for interpreting metabolic plasticity and for supporting the broader use of *O. dancena* in studies of environmental adaptation. The present study therefore aimed to evaluate the integrated physiological responses of *O. dancena* to hypoosmotic (5 ppt), near isosmotic (23 ppt), and hyperosmotic (35 ppt) conditions. Because osmoregulation imposes substantial ATP demand through Na^+/K^+-ATPase (NKA) activity, shifts in energetic allocation are expected to influence key lipid metabolic pathways, particularly mitochondrial β-oxidation (regulated by *ppar-δ* and *cpt1*) and LC-PUFA biosynthesis (*fads2*, *elovl5*). By combining liver histology, whole-body digestive and antioxidant enzyme activity, expression of osmoregulatory and lipid metabolic

genes, and muscle fatty acid profiles, we provide a multidimensional assessment of how salinity-driven osmoregulatory costs interact with metabolic pathways. This integrative characterization offers foundational insight into the osmoregulatory–metabolic strategies of *O. dancena*, supporting its development as a marine model species for studies of environmental adaptation.

2 Materials and methods

2.1 Experimental design and feeding trial

Two-month-old marine medaka (*Oryzias dancena*) with an average body weight of 0.30 ± 0.025 g and total length of 2.5 ± 0.2 cm were procured from the ICAR-CMFRI Vizhinjam Regional Centre and transported to the wet laboratory of ICAR-CMFRI, Kochi, in oxygenated containers. On arrival, fish were disinfected with potassium permanganate ($KMnO_4$) to prevent disease transmission and acclimated for two weeks in 1000 L FRP tanks under continuous aeration. During acclimation, fish were fed CMFRI Varna ornamental feed (38% protein, 9% lipid) three times daily.

Following acclimation, healthy fingerlings of uniform size were randomly distributed into nine glass aquaria (50 L capacity; 35 L water volume) at a density of 15 fish per tank (45 fish/salinity group). The experiment was conducted in a completely randomized design with three salinity treatments: 5 ppt (hypoosmotic stress), 23 ppt (near isosmotic/optimal salinity), and 35 ppt (hyperosmotic stress), each in triplicate. The selection of these levels was based on prior evidence that *O. dancena* performs optimally at 20–25 ppt (Ranjan et al., 2022), making 23 ppt the reference condition, while 5 and 35 ppt represent physiologically challenging extremes. Salinities were achieved by diluting natural seawater (35–37 ppt) with dechlorinated freshwater and adjusting gradually (3–5 ppt day^{-1}). A salinity of 5 ppt was selected instead of 0 ppt freshwater to avoid acute osmotic shock and to better represent ecologically relevant low-salinity conditions experienced by *O. dancena* in estuarine and coastal environments.

Fish were reared for 45 days and fed a formulated diet (40% protein, 10% lipid) to apparent satiation three times daily (09:00, 13:00, 17:00 h). Feed composition and fatty acid profiles are provided in Supplementary file S1. Continuous aeration was supplied to all tanks. Uneaten feed and fecal matter were siphoned out daily, and 25–50% of the water was replaced with pre-adjusted water of the corresponding salinity.

All experimental procedures involving fish, including rearing, handling, and sampling, were reviewed and approved by the Animal Ethics Committee of the Central Marine Fisheries Research Institute, Kochi, India. Every effort was made to minimize fish stress by maintaining optimal rearing conditions. At the end of the trial, fish were anesthetized with clove oil (Himedia, India; 50µL L^{-1}) prior to euthanasia and sampling.

2.2 Sampling

At the end of the 45-day salinity challenge, fish from each treatment were randomly sampled for biochemical, histological, fatty acid, and molecular analyses. Prior to sampling, fish were subjected to 24 h fasting and anesthetized as described above. For histological analysis, liver samples from three fish per tank were excised and immediately fixed in 10% neutral buffered formalin (NBF, Sigma-Aldrich, HT501128). For biochemical assays, whole-body samples were collected from three individual fish per tank (nine fish per treatment). Each fish was processed independently. Whole-body tissues were homogenized in ice-cold sucrose buffer at a 1:19 (w/v) tissue-to-buffer ratio, centrifuged, and the resulting supernatants were stored at −80°C until analysis. For gene expression analysis, liver tissues from three fish per tank were dissected and immediately placed in Eppendorf tubes containing 0.5 mL of RNAlater® (Invitrogen™, Thermo Fisher Scientific; Cat. No. AM7020), kept at 4°C for 24 h, and then stored at -80°C until further processed. For fatty acid analysis, white muscle tissue from three fish per tank was collected individually and stored at −20°C until lipid extraction and fatty acid methyl esters (FAME) preparation.

2.3 Biochemical assay

Digestive, antioxidant, and metabolic enzyme activities were measured using whole-body homogenates. The final body weight of *O. dancena* at the end of the 45-day experimental period was ~0.6 ± 0.1 g, which did not permit reliable and reproducible tissue-specific enzymatic assays with adequate replication. Liver tissue was therefore prioritized exclusively for RNA extraction to ensure sufficient quantity and integrity for gene expression analyses, and the remaining tissue mass was insufficient for parallel, tissue-specific biochemical assays. Accordingly, antioxidant enzymes (superoxide dismutase, catalase, total antioxidant capacity) and metabolic enzymes (aspartate aminotransferase, alanine aminotransferase), as well as digestive enzymes, were assessed using whole-body homogenates to obtain an integrated measure of organism-level physiological responses to salinity stress. This approach is commonly applied in small teleost models, including medaka and zebrafish, for digestive and oxidative enzyme analyses (Guerrera et al., 2015; Yeh et al., 2013; Ramírez-Duarte et al., 2016, 2017). While this method does not resolve tissue-specific enzyme sources, interpretations are accordingly restricted to systemic physiological responses rather than organ-specific regulation.

Protease activity was determined using the casein digestion method (Drapeau, 1976), amylase using the DNS method (Rick and Stegbauer, 1974), and lipase using p-nitrophenyl palmitate as substrate (Katsivela et al., 1995). Protease activity was expressed as µg tyrosine equivalents mg^{-1} protein, lipase activity as µmol p-nitrophenol equivalents mg^{-1} protein, and amylase activity as µg maltose equivalents mg^{-1} protein. Antioxidant enzymes were measured as follows: superoxide dismutase (SOD) using inhibition of epinephrine auto-oxidation (Misra and Fridovich, 1977), catalase (CAT) based on H_2O_2 decomposition (Aebi, 1984), and total antioxidant capacity (TAC) using the phosphomolybdenum method (Prieto et al., 1999). Superoxide dismutase (SOD) and catalase (CAT) activities were expressed as units per minute per milligram of soluble protein (U min^{-1} mg^{-1} protein), while total antioxidant capacity (TAC) was expressed as µg ascorbic acid equivalents per milligram of protein. Metabolic enzymes, including aspartate aminotransferase (AST) and alanine

aminotransferase (ALT), were quantified using IFCC-based diagnostic kits (Coral Clinical Systems, India; AST Cat. No. 10707001; ALT Cat. No. 10701001). AST and ALT activities were expressed as units per minute per milligram of soluble protein (U min^{-1} mg^{-1} protein). All enzyme activities were normalized to soluble protein concentration. Protein concentration was determined using the Bradford method, and no significant differences in total soluble protein content were observed among salinity treatments. All enzyme assay analyses were in triplicate with a control and a blank to ensure analytical precision.

2.4 Gene expression

Total RNA was extracted from liver tissues using RNAiso Plus (Takara Bio Inc., Japan; Cat. No. 9109) following the manufacturer's instructions. RNA concentration and purity were assessed using a Nano Drop spectrophotometer (Thermo Fisher Scientific, USA). Equal amounts of RNA (500 ng per sample) were used for first-strand cDNA synthesis with the PrimeScript™ 1st Strand cDNA Synthesis Kit (Takara Bio Inc., Japan; Cat. No. 6110A), which included a genomic DNA elimination step. The synthesized cDNA was stored at −20°C until further use.

The mRNA expression levels of *fads2*, *elovl5*, *ppar-δ*, *cpt1*, and *nka* were quantified by quantitative real-time PCR (qPCR). Primers (Table 1) were designed with Primer3 software (v.0.4.0; https://primer3.ut.ee/) based on available GenBank sequences: *fads2 (Oryzias dancena;* PP957852*) elovl5 (O.dancena;* PP957853*), ppar-δ (O.latipes;* XM_023956218.1*), cpt1 (O.latipes;* XM_004071865.4*), nka (O.dancena;* EU490421*) and β-actin (O.dancena;* EU490422*).* For *ppar-δ* and *cpt1*, primers were designed using *O. latipes* sequences because annotated sequences for these genes are not yet available for *O. dancena*; *O. latipes* is a closely related congeneric species with high sequence conservation. For cross-species primers, sequence identity was confirmed through BLAST alignment against *Oryzias* spp. sequences. Primer specificity was further validated by conventional PCR, which yielded single expected-size amplicons, as well as by single-peak melt curves. Primer efficiency was validated using standard curves generated from serial dilutions of pooled cDNA, and only primers with efficiencies between 90–110% were used (Tine, 2017). Quantitative PCR reactions were performed on an AriaMx Real-Time PCR System (Agilent Technologies, Singapore) in 20 µL volumes containing 10 µL SYBR Green Supermix (Takara Bio Inc., Japan; Cat. No. RR820A), 1 µL of each primer, 7 µL of nuclease-free water, and 1 µL of cDNA template. The amplification program consisted of an initial denaturation at 95°C for 3 min, followed by 35 cycles of 95°C for 30 s, 60°C for 30 s, and 72°C for 30 s. A melt-curve analysis was included at the end of each run to confirm single-product amplification. Relative expression levels were calculated using the efficiency-corrected Pfaffl method (Pfaffl, 2001). β-actin was used as the reference gene. The stability of β-actin expression across salinity treatments was statistically validated using Shapiro–Wilk tests for normality, Levene's test for homogeneity of variances, and one-way ANOVA, with no significant differences detected among treatments ($P > 0.05$; Supplementary file S2). Although the use of multiple reference genes is generally recommended, single-gene normalization has been widely applied in teleost qPCR studies when a stably expressed reference gene is used for normalization (Pfaffl, 2001; Pfaffl et al., 2004; Huggett et al., 2005; Li et al., 2010, 2020; Satkar et al., 2025). Normalized expression values were used for statistical comparison.

2.5 Fatty acid analysis

Muscle lipids were extracted using the Bligh and Dyer method (1959), with modifications after Manirakiza et al. (2001). Samples were homogenized in chloroform–methanol–water (2:1:0.2, v/v/v) under nitrogen, shaken, incubated at 4°C, and phase-separated with saturated NaCl. The organic layer was dried over anhydrous sodium sulfate, filtered, concentrated by rotary evaporation (40°C), and dried under nitrogen. Lipids were converted to FAMEs using methanolic boron trifluoride (Metcalfe et al., 1966).

FAMEs were analyzed on a gas chromatograph (PerkinElmer Autosystem XL, USA) fitted with an Elite 225 capillary column

TABLE 1 Primers used for real-time quantitative PCR (qPCR).

Primers	Sequence	Amplicon size	Efficiency (%)	GenBank accession no.	Reference
fads2	F-GGGTGGATTTGGCGTGGTAT	122	107	PP957852.1	Self-designed
	R-CCAGTGACTCTCCAGGAACC				
elovl5	F-CTCCGGCCTTATCTGTGGTG	151	101	PP957853.1	Self-designed
	R-TCGTGCCCATGTAGCTGATC				
ppar-δ	F-GCAGGTGGAACAGAGTCAGG	156	102	XM_023956218.1	Self-designed
	R-AGTAGAGGGTGGAGCGAGGT				
cpt1	F-TGGGGTCAACAAAAGGTCTC	200	105	XM_004071865.4	Self-designed
	R-CGCTCTTCCCGTTCTTGTAG				
nka	F- GGAAGACAGCTACGGACAGC	135	98	EU490421.1	(Kang et al., 2008)
	R-GAGTTCCTCCTGGTCTTGCA				
β-actin	F-GGAAATCGTGCGTGACATCA	188	110	EU490422.1	Self-designed
	R-TACCAAGGAATGAGGGCTGG				

fads2, Δ6 fatty acid desaturase2; *elovl5*, elongation of very long chain fatty acid5; *ppar-δ*, peroxisome proliferator receptor-delta; *cpt1*, carnitine palmitoyltransferase1; *nka*, Na^+/K^+-ATPase; *β-actin*-beta actin.

(30 m × 0.25 mm × 0.25 μm) and a flame ionization detector. Nitrogen served as the carrier gas (0.5 ml min^{-1}). The oven program was 110°C to 240°C (2.7°C min^{-1}), held 3 min, then raised to 280°C and held 5 min. Fatty acids were identified by comparison with a Supelco 37 Component FAME Mix (Sigma-Aldrich, USA; Cat. No. 47885), and results expressed as relative percentage of total identified FAMEs.

2.6 Histology

Fresh livers were collected and fixed in a 10% neutral formalin buffer solution. The samples were then dehydrated in a graded alcohol series, cleared in xylene (Auto-Tissue processor (Leica TP1020), paraffin-embedded (Thermo Electron Corporation; Shandon Histocentre 3), sectioned at 3μm (Leica RM2125 RTS, Germany), and stained with hematoxylin and eosin (H&E) with slight modification based on tissue. Sections were then examined under a microscope (Nikon Eclipse 80i). The vacuolization measured in terms of the number and size of vacuoles (Gora et al., 2022, 2023) was analyzed using the ImageJ software (Schneider et al., 2012).

2.6 Statistical analysis

For all biochemical assays, gene expression, histology, and fatty acid profile, three individual fish were sampled from each of the three tanks per salinity group, yielding nine independent biological replicates per treatment (n = 9). Data were first checked for normality using the Shapiro–Wilk test and for homogeneity of variances using Levene's test. Differences among salinity treatments were assessed using one-way ANOVA followed by Tukey's HSD *post hoc* test when significant effects were detected ($P < 0.05$). All statistical analyses were performed using GraphPad Prism 8.0 (GraphPad Software Inc., San Diego, CA, USA).

3 Results

3.1 Biochemical analysis

The activities of digestive, antioxidant, and metabolic enzymes in *Oryzias dancena* exposed to different salinities are given in Figures 1–3, respectively. Protease activity was significantly higher ($P < 0.05$) at 5 ppt compared to 35 ppt, while fish maintained at 23 ppt showed intermediate values. Lipase activity peaked at 23 ppt ($P < 0.05$) relative to 5 ppt and 35 ppt, whereas amylase activity did not differ significantly among treatments. Superoxide dismutase (SOD) activity was significantly elevated at 5ppt compared to 35 ppt, with intermediate values observed for 23 ppt. In contrast, catalase (CAT) activity and total antioxidant capacity (TAC) did not differ significantly among salinity treatments (Figure 2). The activity of metabolic enzymes aspartate aminotransferase (AST) and alanine aminotransferase (ALT) did not differ significantly across treatments, as shown in Figure 3. Although not statistically significant, AST activity was numerically higher at 5 ppt, whereas ALT activity was numerically higher at 35 ppt.

3.2 Histology

Histological examination of the liver section showed salinity-induced alteration in hepatocellular morphology of *Oryzias dancena*. Fish reared at 5 ppt exhibited macrovesicular steatosis characterized by large, irregular vacuoles, with nuclei displaced toward the cell periphery. Similarly, fish at 35 ppt displayed prominent vacuolization. In contrast, livers of fish at 23ppt showed comparatively mild hepatic changes with smaller vacuoles and nuclei located in the central or slightly displaced the hepatic architecture at 23 ppt appeared closer to normal, in terms of vacuole size and number, suggesting reduced metabolic stress compared with hypo- and hypersaline conditions (Figure 4).

3.3 Gene expression

The expression of key genes associated with lipid metabolism and osmoregulation was assessed using qPCR. Expression levels of *fads2* and *elovl5*, encoding fatty acid desaturase 2 and elongase of very long-chain fatty acids 5, respectively, did not differ significantly across salinity treatments, indicating that LC-PUFA biosynthetic gene regulation remained stable under the tested conditions. In contrast, *ppar-δ* expression was significantly elevated at 23 ppt compared with both 5 and 35 ppt, suggesting enhanced lipid oxidative activity under near-iso-osmotic conditions. Similarly, *cpt1*, a marker of mitochondrial β-oxidation, was upregulated at 23 and 35 ppt relative to 5 ppt. Expression of the osmoregulatory gene *nka* (Na^+/K^+-ATPase) was significantly higher under both hypo- and hypersaline conditions (5 and 35 ppt) compared with 23 ppt, consistent with greater osmoregulatory demand at salinity extremes (Figure 5).

3.4 Fatty acid composition

The muscle fatty acid (FA) composition of *Oryzias dancena* is presented in Table 2. Saturated fatty acids (SFA), predominantly palmitic acid (C16:0), accounted for 32.6–34.5% of total FA and did not vary significantly across salinity treatments. Monounsaturated fatty acids (MUFA) were dominated by oleic acid (C18:1n9c), which remained stable (~28–30%). However, palmitoleic acid (C16:1) was significantly higher at 35 ppt (7.3%) compared to 5–23 ppt (~4.4%). Consequently, ΣMUFA was elevated at 35 ppt (36.79%). Among polyunsaturated fatty acids (PUFA), n-6 PUFA (15–17%) showed no significant variation, although arachidonic acid (ARA, C20:4n6) was lower at 23–35 ppt relative to 5 ppt. n-3 PUFA ranged between 11.3–13.6%, with α-linolenic acid (C18:3n3) and EPA (C20:5n3) remaining stable. Notably, docosahexaenoic acid (DHA, C22:6n3) declined significantly at 35 ppt (3.4%) compared to 5–23 ppt (5.8–5.9%). This selective reduction in DHA under hyperosmotic conditions may indicate its sensitivity to osmotic stress, supporting its potential use as a physiological biomarker in future studies.

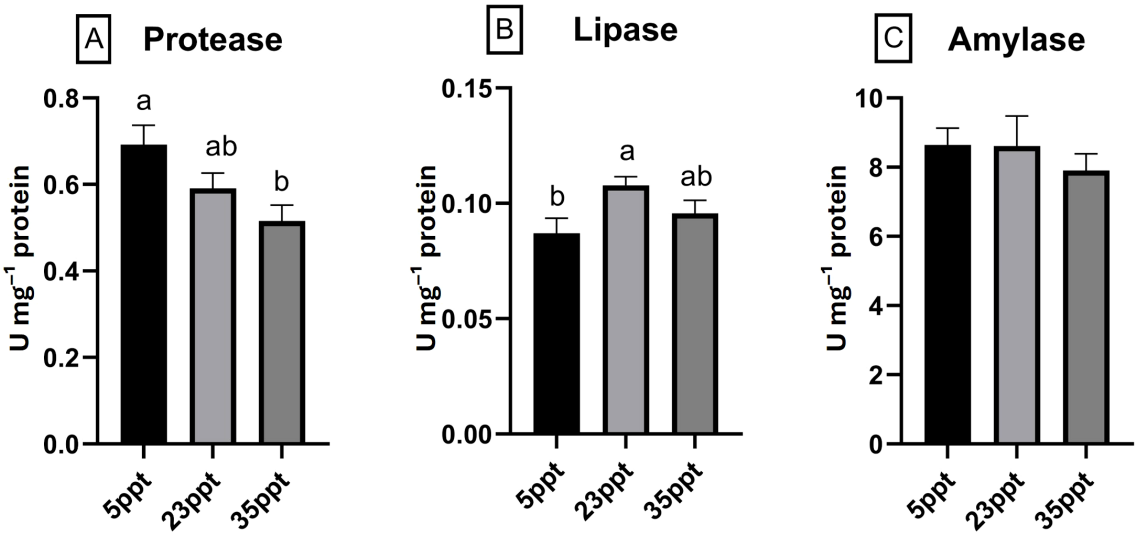

FIGURE 1
Digestive enzyme activities measured in whole-body homogenates of *Oryzias dancena* reared under different salinity conditions. **(A)** Protease, **(B)** Lipase, **(C)** Amylase. Different letters indicate statistically significant differences among treatments based on one-way ANOVA followed by Tukey's multiple comparisons test ($P < 0.05$). Data are expressed as mean ± SEM (n = 9). Protease activity is expressed as μg tyrosine equivalents mg^{-1} protein, lipase activity as μmol p-nitrophenol equivalents mg^{-1} protein, and amylase activity as μg maltose equivalents mg^{-1} protein.

4 Discussion

Water salinity is a major abiotic driver of energy metabolism in euryhaline fishes, where the liver plays a central role in coordinating lipid storage and mobilization under osmotic stress (Evans and Kültz, 2020; Kültz, 2015; Tseng and Hwang, 2008). In the present study, salinity variation induced distinct changes in hepatic lipid morphology, gene expression, enzyme activity, and muscle fatty acid composition in *Oryzias dancena*.

Hepatic vacuole morphology proved highly sensitive to salinity fluctuations in *Oryzias dancena*. At 5 ppt, fish exhibited macrovesicular steatosis, characterized by numerous irregularly shaped vacuoles and displaced nuclei, indicating disrupted lipid packaging and hepatocellular stress. Similar histopathological alterations under osmotic extremes have been reported in other teleosts, where exposure to hypo- and hyperosmotic conditions caused hepatocellular vacuolization, irregular nuclear positioning, and disrupted tissue architecture (Xiao et al., 2022; Fridman, 2020).

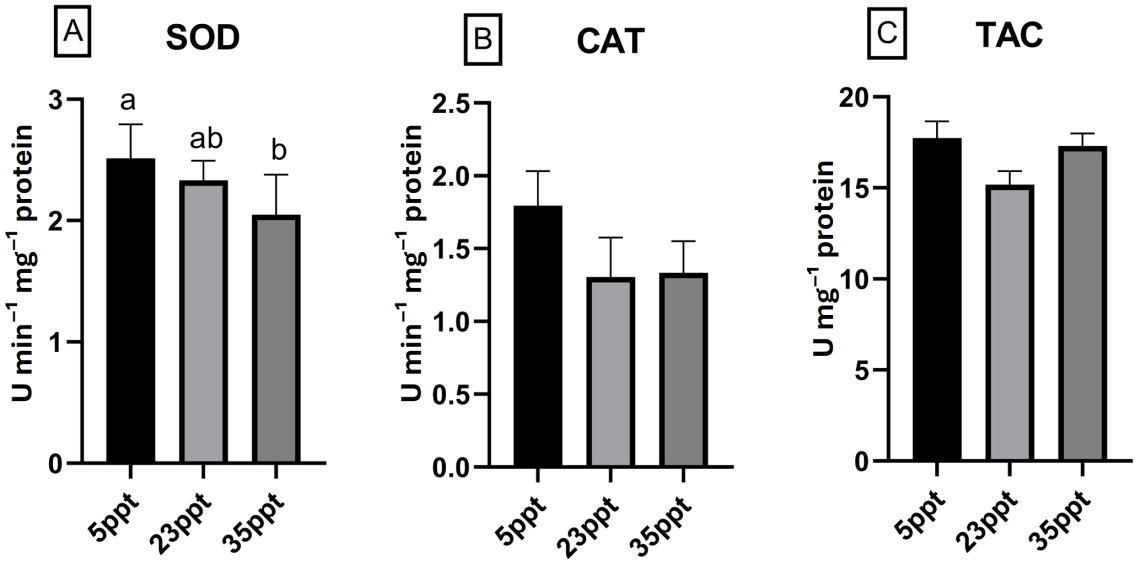

FIGURE 2
Antioxidant enzyme activities measured in whole-body homogenates of *Oryzias dancena* reared under different salinity conditions. **(A)** Superoxide dismutase (SOD), **(B)** Catalase (CAT), **(C)** Total Antioxidant Capacity (TAC). Different letters denote statistically significant differences among treatments based on one-way ANOVA with Tukey's *post hoc* test ($P < 0.05$). Data are expressed as mean ± SEM (n = 9). SOD and CAT activities are expressed as U min^{-1} mg^{-1} protein, and TAC is expressed as μg ascorbic acid equivalents mg^{-1} protein.

10.3389/fmars.2026.1716162

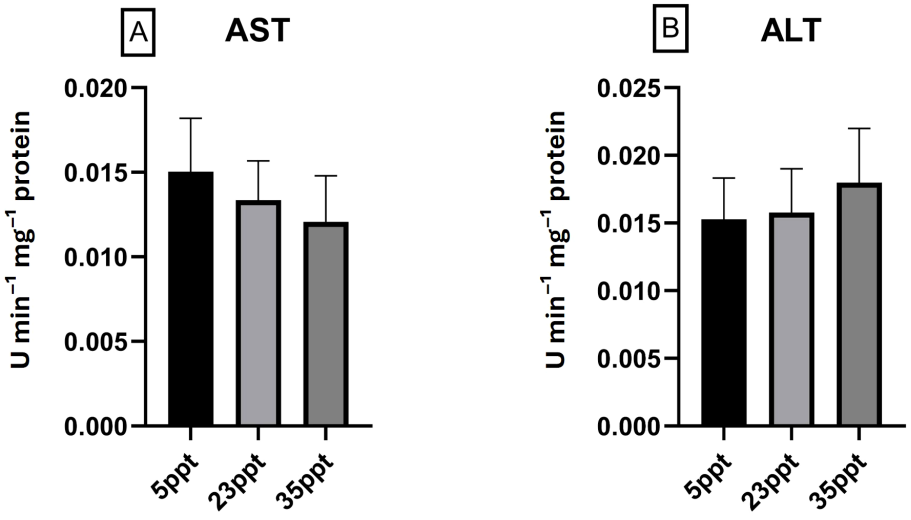

FIGURE 3
Metabolic enzyme activities measured in whole-body homogenates of *Oryzias dancena* reared under different salinity conditions. **(A)** Aspartate aminotransferase (AST), **(B)** Alanine aminotransferase (ALT). No statistically significant differences were detected among treatments (one-way ANOVA, $P > 0.05$). Values shown as mean ± SEM (n = 9). AST and ALT activities are expressed as U min^{-1} mg^{-1} protein.

In contrast, at 23 ppt, vacuoles were smaller and more uniform, suggesting efficient lipid turnover and a reduced metabolic load, consistent with optimal metabolic homeostasis at near-iso-osmotic conditions. The observed hepatic responses are consistent with established models of euryhaline fish adaptation, which rely on tissue-specific strategies to manage ionic and energetic demands in fluctuating environments (Varsamos et al., 2005). These results highlight the liver's dynamic role in responding to environmental salinity shifts, where vacuolar changes are a key indicator of metabolic and osmotic stress. This adaptive mechanism may reflect a trade-off between energy storage and membrane structural integrity under high salinity. Such morphological plasticity is critical for maintaining hepatocyte function and overall cellular homeostasis, as the liver plays a central role in lipid metabolism and osmoregulation in euryhaline teleosts (Evans, 2008; Kültz, 2015).

Digestive and antioxidant enzyme activities reflected salinity-dependent metabolic adjustments in *Oryzias dancena*. Protease activity was significantly higher at 5 ppt, likely indicating enhanced protein digestion to meet the demands of hypoosmotic stress, consistent with reports in hybrid grouper (*Epinephelus* spp.; Sutthinon et al., 2015) and golden-line seabream (*Rhabdosargus sarba*; Woo and Kelly, 1995). However, despite this active protein catabolism, poor lipid metabolism at low salinity was apparent, evidenced by fat accumulation within tissues as vacuoles in histological sections. This may suggest an inefficiency in utilizing stored lipids for energy at low salinity, contributing to lipid storage despite elevated protein breakdown. Conversely, lipase activity peaked at 23 ppt, the near-iso-osmotic condition, indicating more efficient lipid digestion and utilization. Lipases catalyze the hydrolysis of triglycerides into free fatty acids and glycerol, which serve as key energy substrates for mitochondrial β-oxidation. The observed increase in *ppar-δ* and *cpt1* gene expression at 23 ppt supports the activation of lipid metabolism regulatory pathways in this condition. This coordinated upregulation suggests that moderate salinity (23 ppt) provides the most metabolically favorable environment for lipid utilization as an energy source. In contrast, amylase activity remained consistent across salinity treatments, indicating that carbohydrate digestion was not significantly influenced by salinity variation. This is consistent with Liu et al. (2017), who found no significant effect of salinity on amylase activity in juvenile American shad (*Alosa sapidissima*), supporting the idea that teleost fish exhibit relatively low plasticity in carbohydrate metabolism compared to lipids.

Antioxidant enzyme responses in whole-body homogenates also reflected stress at salinity extremes. In the present study, elevated superoxide dismutase (SOD) and catalase (CAT) activity at 5 ppt, together with increased total antioxidant capacity (TAC) at both 5 ppt and 35 ppt, suggest activation of reactive oxygen species (ROS) scavenging pathways to counteract oxidative stress (Sinha et al., 2015; Atli and Canli, 2008). Similar organism-level antioxidant responses assessed using whole-body homogenates have been reported in medaka models. For instance, Ramírez-Duarte et al. (2016, 2017) quantified SOD and CAT activities in whole-body homogenates of *Oryzias latipes* under environmental stress, demonstrating that whole-body antioxidant enzyme measurements provide robust indicators of systemic oxidative status in small teleosts. Similarly, tissue-specific oxidative responses have been reported in other euryhaline teleosts. Jiang et al. (2022) demonstrated significantly elevated SOD and CAT activities in gill tissues of silver carp (*Hypophthalmichthys molitrix*) under hypoosmotic stress, whereas antioxidant enzyme responses in kidney tissue were weaker or non-significant. Furthermore, although differences in aspartate aminotransferase (AST) and alanine aminotransferase (ALT) activities were not statistically significant in the present study, AST activity was numerically higher at 5 ppt, while ALT activity tended to increase at 35 ppt. As ALT is predominantly associated with hepatic metabolism (Koper et al., 2022), comparable increases in serum AST and ALT have been reported in Nile tilapia (*Oreochromis niloticus*) exposed to salinity stress, reflecting metabolic challenge at osmotic extremes (Metwaly et al., 2025; Motamedi-Tehrani et al., 2025). Together, these findings align with the observed enlargement and

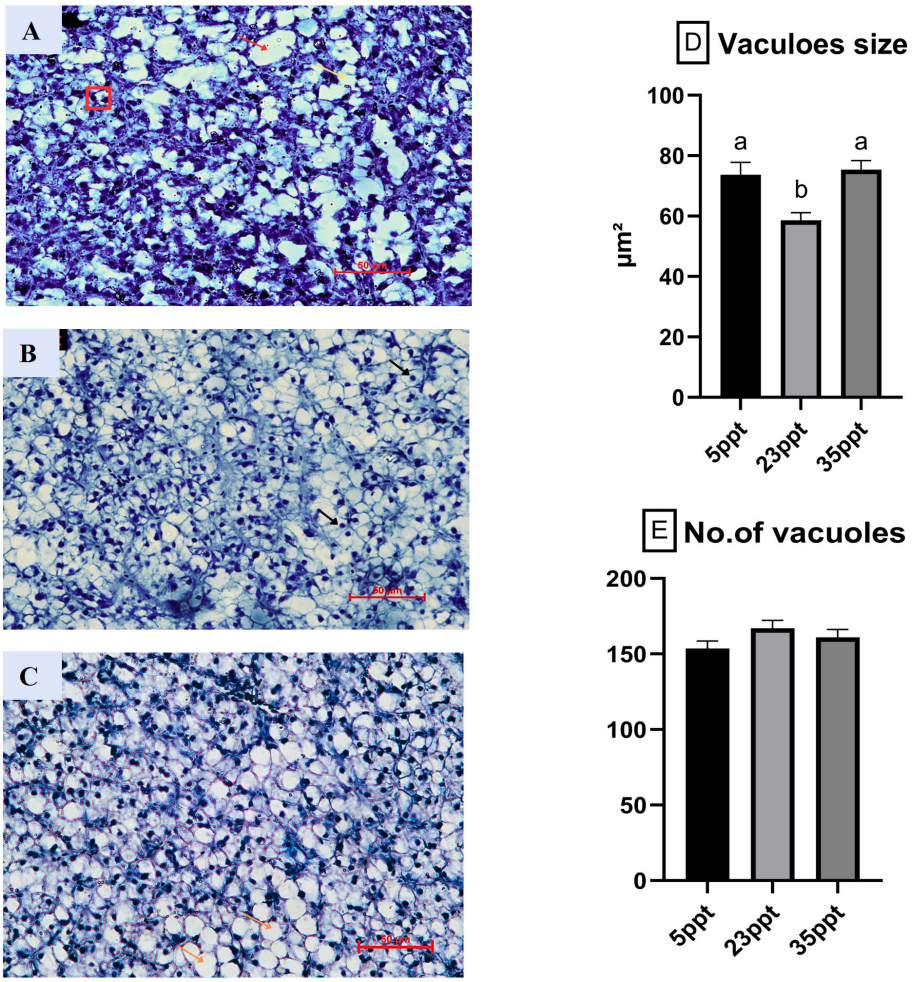

FIGURE 4
A representative liver histological section of *Oryzias dancena* under different salinities (5, 23, and 35 ppt) (H&E stain, 40X). **(A)** 5ppt, the red arrows show very large vacuoles, the yellow arrows show both small and large vacuoles, and the rectangular box shows the displacement of nuclei to the cell periphery in the liver cells. **(B)** 23 ppt, the black arrows show small vacuoles in the liver cells. Some cells have the nucleus in the centre or slightly to the side, showing mild fat accumulation. **(C)** 35ppt, the orange arrows show large vacuoles and uniform size and shape. The vacuole size **(D)** and Number of vacuoles **(E)** were analysed using ImageJ software. Different letters denote statistically significant differences among treatments based on one-way ANOVA with Tukey's *post hoc* test ($P < 0.05$). Data are expressed as mean ± SEM (n = 9).

irregularity of hepatic lipid vacuoles at 5 and 35 ppt, suggesting that salinity-induced oxidative and metabolic stress may contribute to disrupted hepatic lipid homeostasis under osmotic extremes.

Gene expression profiles provided mechanistic insights into these histological observations. In the present study, upregulation of hepatic Na^+/K^+-*ATPase (nka)* at 5 ppt and 35 ppt indicates higher energetic costs for active ion transport under hypo- and hyperosmotic stress, consistent with earlier findings in *O. dancena* and other euryhaline models (Kang et al., 2008; Kültz, 2015; Chandrasekar et al., 2014; Lin et al., 2004). In contrast, hepatic *nka* expression was lowest at 23 ppt, reflecting reduced osmoregulatory effort at near-iso-osmotic salinity. Similar biphasic responses have been reported in other euryhaline teleosts at the tissue level. For example, branchial *nka* expression and activity were elevated under both low and high salinities in *Etroplus suratensis*, showing a characteristic U-shaped response to salinity (Chandrasekar et al., 2014). Collectively, these findings emphasize *nka* as a conserved central regulator of ion transport and energy expenditure in salinity adaptation, with biphasic elevation reflecting increased energetic investment to counter ion loss at low salinity and ion gain at high salinity (Kültz, 2015; Kang et al., 2008).

In the present study, *fads2* and *elovl5*, encoding key enzymes in LC-PUFA biosynthesis, did not differ significantly across salinity treatments, indicating that major shifts in LC-PUFA biosynthesis were not evident at the transcriptional level under the tested conditions, even though other euryhaline species (e.g., red tilapia) have shown salinity-dependent modulation of these genes (Yu et al., 2021; Tocher et al., 2006; Chen et al., 2023). In contrast to the stable expression of *fads2* and *elovl5*, upregulation of *ppar-δ* and *cpt1* at 23 ppt reflects enhanced mitochondrial β-oxidation and lipid turnover, aligning with the smaller vacuole size and suggesting optimal metabolic efficiency at near-iso-osmotic salinity. This trade-off between lipid synthesis and oxidation across salinity regimes highlights the metabolic plasticity of euryhaline fishes (Jin et al., 2025; Marrero et al., 2021; Si YuFeng et al., 2018; Torres-Rodríguez et al., 2025). The downregulation of *cpt1* at 5 ppt further suggests a metabolic shift away from lipid catabolism, likely reflecting prioritization of energy toward osmoregulatory functions or

10.3389/fmars.2026.1716162

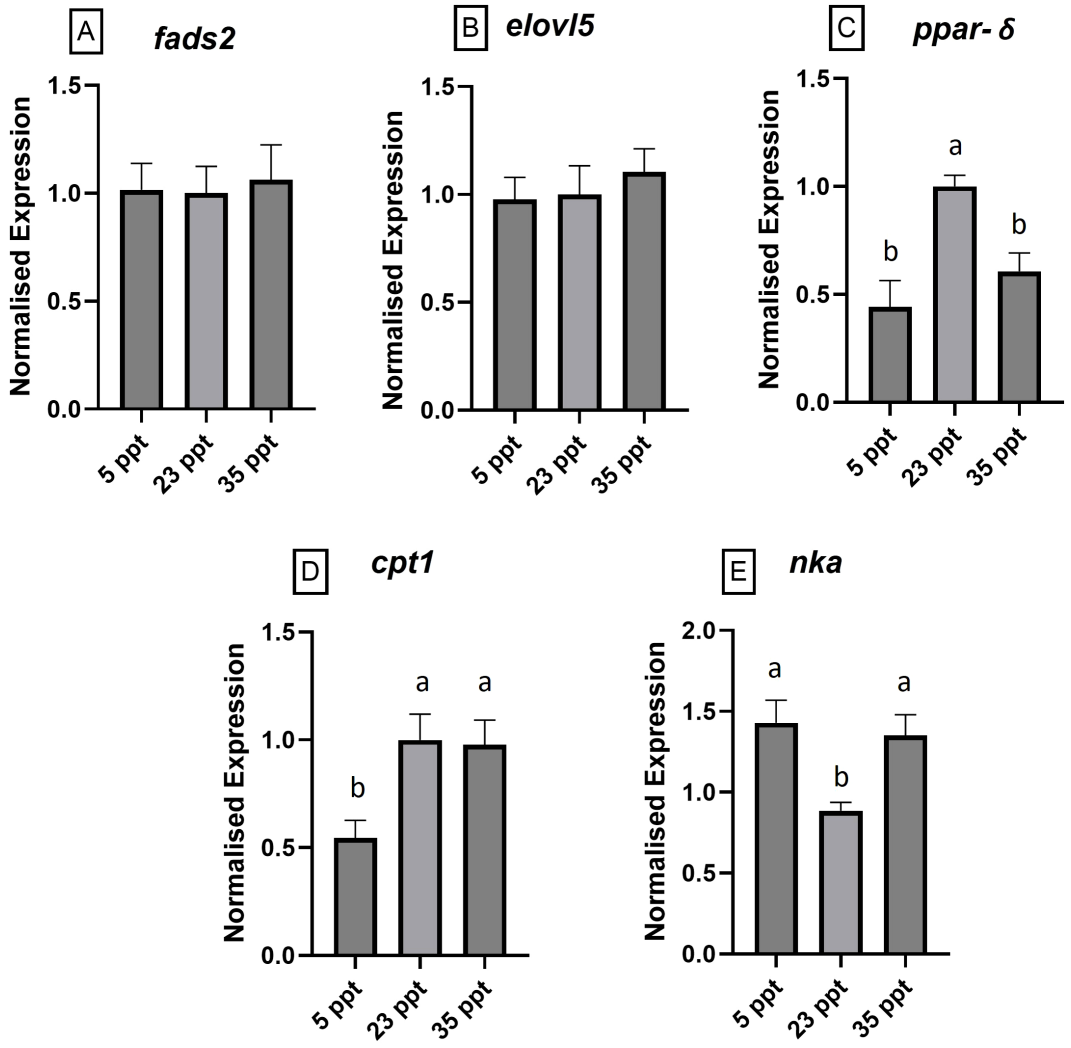

FIGURE 5
Hepatic mRNA expression of osmoregulatory and lipid metabolic genes in *Oryzias dancena* reared under different salinity conditions. **(A)** *fatty acid desaturase 2 (fads2)*, **(B)** *elongase of very long-chain fatty acids 5 (elovl5)*, **(C)** *peroxisome proliferator-activated receptor-delta (ppar-δ)*, **(D)** *carnitine palmitoyltransferase 1 (cpt1)*, **(E)** *Na^+/K^+-ATPase (nka)*. Different letters indicate statistically significant differences among treatments based on one-way ANOVA followed by Tukey's multiple comparisons ($P < 0.05$). Data are expressed as mean ± Standard error mean (SEM), n = 9.

impaired efficiency under cellular stress. Collectively, the gene expression profiles reflect a coordinated regulatory mechanism whereby *O. dancena* enhances ion transport under salinity stress, while lipid catabolism is favoured under homeostatic conditions. These molecular responses align with liver histological observations, wherein higher vacuolization was observed at salinity extremes, suggesting altered lipid turnover, whereas smaller, regular vacuoles at 23 ppt indicate efficient lipid utilization and metabolic homeostasis. Comparable salinity-driven metabolic trade-offs have been reported in several economically important euryhaline teleosts, reinforcing the broader physiological relevance of the present findings. In *Etroplus suratensis*, branchial Na^+/K^+-ATPase activity and energy expenditure increase under both hypo- and hyperosmotic conditions, reflecting elevated osmoregulatory costs similar to those observed in *O. dancena* (Chandrasekar et al., 2014). Likewise, studies in Nile tilapia (*Oreochromis niloticus*) demonstrate salinity-dependent modulation of hepatic metabolism, antioxidant defenses, and lipid utilization, with near-iso-osmotic salinities supporting improved metabolic efficiency (Metwaly et al., 2025; Motamedi-Tehrani et al., 2025). In marine and estuarine species such as gilthead seabream (*Sparus aurata*), sole (*Solea senegalensis*), and Japanese sea bass (*Lateolabrax japonicus*), salinity has been shown to alter lipid oxidation capacity and tissue fatty acid composition, including DHA dynamics, highlighting conserved energetic strategies across euryhaline taxa (Imsland et al., 2001; Dong et al., 2020; Marrero et al., 2021). Together, these comparisons indicate that the metabolic patterns observed in *O. dancena* align with established responses in commercially relevant species, supporting its suitability as a model for studying salinity-driven physiological and metabolic adaptation with relevance to aquaculture and fisheries biology.

Muscle fatty acid (FA) profiles were largely conserved across salinities, indicating strong homeostatic control over membrane lipid composition. However, at 35 ppt, DHA (22:6n3) content declined significantly, accompanied by an increase in monounsaturated fatty acids (MUFA), particularly palmitoleic acid (C16:1). Given DHA's critical role in maintaining membrane

10.3389/fmars.2026.1716162

TABLE 2 Fatty acid composition (percentage of total fatty acids) of the muscle of *Oryzias dancena* reared under different salinity conditions.

Fatty acids	5ppt	23ppt	35ppt
C14:0 (Myristic)	2.00 ± 0.14	1.85 ± 0.19	2.08 ± 0.05
C16:0 (Palmitic)	22.76 ± 0.64	24.44 ± 0.25	22.98 ± 0.52
C18:0 (Stearic)	7.13 ± 0.04	7.37 ± 0.22	7.13 ± 0.07
C20:0 (Arachidic)	0.75 ± 0.02	0.79 ± 0.05	0.82 ± 0.02
ΣSFA	32.63 ± 0.75	34.46 ± 0.39	33.00 ± 0.55
C16:1 (Palmitoleic)	4.33 ± 0.08 ^{b}	4.52 ± 0.15 ^{b}	7.29 ± 0.54 ^{a}
C18:1n9c (Oleic)	29.60 ± 0.17^{a}	28.25 ± 0.27^{b}	29.01 ± 0.44^{a}
C20:1n9 (cis-11-Eicosenoic)	0.49 ± 0.14	0.50 ± 0.07	0.50 ± 0.10
ΣMUFA	34.42 ± 0.39	33.26 ± 0.08	36.79 ± 0.85
C18:2n6c (Linoleic)	15.47 ± 0.64	16.02 ± 0.35	16.18 ± 0.26
C18:3n6 (γ-Linolenic)	0.37 ± 0.07	0.38 ± 0.02	0.37 ± 0.04
C20:4n6 (Arachidonic)	1.53 ± 0.23	1.16 ± 0.10	1.28 ± 0.03
Σn-6 PUFA	17.37 ± 0.43	17.55 ± 0.32	17.82 ± 0.30
C18:3n3 (α-Linolenic)	6.44 ± 0.53	6.12 ± 0.21	6.44 ± 0.25
C20:3n3 (cis-11,14,17-Eicosatrienoic)	0.34 ± 0.01	0.32 ± 0.03	0.34 ± 0.03
C20:5n3 (cis-5,8,11,14,17-Eicosapentaenoic)	1.11 ± 0.07	1.23 ± 0.06	1.18 ± 0.09
C22:6n3 (cis-4,7,10,13,16,19-Docosahexaenoic)	5.88 ± 0.25^{a}	5.80 ± 0.25^{a}	3.38 ± 0.31^{b}
Σn-3 PUFA	13.76 ± 0.76^{a}	13.47 ± 0.36^{a}	11.34 ± 0.24^{b}

SFA-saturated fatty acids, MUFA-Monounsaturated fatty acids, PUFA-poly unsaturated fatty acids.
Different letters indicate statistically significant differences among treatments based on nested one-way ANOVA followed by Tukey's multiple comparisons ($P < 0.05$). The data are expressed as mean ± Standard error mean (SEM), n = 3.
Bold values represent the summed fatty acid classes (ΣSFA, ΣMUFA, ΣPUFA, Σn-6 PUFA and Σn-3 PUFA).

fluidity and supporting cellular signalling (Sargent et al., 2003), its depletion under hyperosmotic stress suggests a degree of metabolic vulnerability, potentially reflecting increased DHA utilization for membrane stabilization or limited substrate availability. This phenomenon has also been reported in tilapia and salmonids exposed to salinity challenge (Tocher, 2003; Morais et al., 2011). In contrast, several studies have reported the marked increases in EPA and DHA in response to elevated salinities in different fish species, including Japanese sea bass (*Lateolabrax japonicus*) (Dong et al., 2020), black seabream (*Acanthopagrus schlegelii*) (Li et al., 2022), sole (*Solea senegalensis*) (Marrero et al., 2021), largemouth bass (*Micropterus salmoides*) (Du et al., 2022), blue tilapia (Zhou et al., 2024), and *Fundulus heteroclitus* (Torres-Rodríguez et al., 2025). These contradictory patterns likely reflect species-specific lipid regulatory strategies, differences in dietary input, experimental conditions, or tissue-specific biosynthetic versus utilization balance (Tocher, 2010; Monroig et al., 2013). In the present study, the lack of significant changes in *fads2* and *elovl5* suggests that the reduced DHA at 35 ppt was not compensated by increased LC-PUFA biosynthesis, implying that DHA depletion likely reflects oxidative utilization or remodeling demands rather than enhanced synthesis. Alternatively, muscle tissue may prioritize structural lipid stability over adaptive remodelling, leading to selective DHA depletion as an unavoidable metabolic cost during osmotic stress.

Interestingly, the observed increase in palmitoleic acid (C16:1n-7) at 35 ppt may reflect a compensatory membrane remodeling strategy to maintain fluidity and function when DHA is limiting. Supporting this, a recent preprint study on *Fundulus heteroclitus* reported that palmitoleic acid accumulated most at 60 ppt in neural tissues, likely contributing to membrane structural stability under hyperosmotic stress (Torres-Rodríguez et al., 2025). Furthermore, the concurrent accumulation of MUFAs aligns with histological observation of enlarged hepatic lipid vacuoles at high salinity, indicating a metabolic shift toward neutral lipid storage.

Notably, despite the selective depletion of DHA, the stability of EPA (C20:5n3), ARA (C20:4n6), and the n-3/n-6 ratio suggests that *O. dancena* prioritizes the essential fatty acid balance, likely to preserve membrane integrity and cellular performance during osmotic challenges. Similar maintenance of fatty acid balance was reported in gilthead seabream (*Sparus aurata*) under varying salinities, where the n-3/n-6 ratio remained constant despite changes in individual fatty acids (Marrero et al., 2021), underscoring the regulatory importance of conserving this balance. Together, these findings highlight the complex interplay between environmental salinity and lipid homeostasis in euryhaline teleosts. The selective DHA depletion, stability of EPA/ARA/n-3-n-6 balance, and compensatory MUFA accumulation underscore a multifaceted strategy enabling *O. dancena* to cope with osmotic extremes, with DHA emerging as a potential biomarker of hyperosmotic stress and a metabolically sensitive fatty acid during salinity adaptation. As muscle fatty acids alone cannot resolve tissue-specific lipid remodeling, future work should incorporate direct hepatic fatty acid profiling to determine whether DHA depletion reflects altered synthesis, utilization, or redistribution during salinity stress.

5 Conclusion

The present study demonstrates that *Oryzias dancena* exhibits distinct tissue-specific responses to environmental salinity. Hepatic histology and gene expression revealed that salinity extremes (5 and 35 ppt) are associated with altered lipid storage dynamics, elevated osmoregulatory demand as indicated by *nka* expression, and reduced indicators of lipid oxidation capacity, whereas near-iso-osmotic salinity (23 ppt) promotes more efficient lipid utilization, reflected in smaller hepatic vacuoles and higher *ppar-δ* and *cpt1* expression. In contrast, muscle fatty acid composition remained largely conserved, except for DHA depletion at 35 ppt, suggesting a metabolically sensitive response to hyperosmotic stress. This selective reduction highlights DHA as a potential biomarker of salinity-induced metabolic strain in euryhaline teleosts. Although hepatic fatty acid profiling was not performed, the combined assessment of hepatocellular vacuolization, muscle fatty acid patterns, and transcriptional markers of lipid metabolism provides coherent evidence of salinity-associated adjustments in hepatic lipid handling. Overall, this study provides foundational evidence supporting *Oryzias dancena* as a useful euryhaline model for studying salinity-driven physiological and metabolic processes, complementing established laboratory species such as zebrafish. Future work should incorporate direct hepatic fatty acid profiling to resolve synthesis–utilization trade-offs and clarify the mechanistic basis of lipid homeostasis under salinity stress.

Data availability statement

The raw data supporting the conclusions of this article will be made available by the authors, without undue reservation.

Ethics statement

The animal study was approved by ICAR-Central Marine Fisheries Research Institute, Kochi, India. The study was conducted in accordance with the local legislation and institutional requirements.

Author contributions

MA: Formal analysis, Investigation, Writing – original draft. CS: Conceptualization, Data curation, Funding acquisition, Project administration, Supervision, Writing – original draft. TS: Formal analysis, Writing – review & editing. KN: Formal analysis, Writing – review & editing. LP: Project administration, Writing – review & editing. DE: Writing – review & editing. AG: Validation, Writing – review & editing. SP: Formal analysis, Writing – review & editing. AG: Writing – review & editing. TS: Formal analysis, Writing – review & editing. CP: Writing – review & editing. KC: Resources, Writing – review & editing.

Funding

The author(s) declared that financial support was received for this work and/or its publication. The work was performed under the project "*Nutrition and Nutri-genomics Research in Mariculture and Marine Fisheries* (MBT/NGM/24)" funded by ICAR-Central Marine Fisheries Research Institute.

Acknowledgments

The study was conducted under the institute project (MBT/NGM/24), supported by the Indian Council of Agricultural Research, Department of Agriculture, Research and Education, Government of India. The authors sincerely thank the Director, ICAR–Central Marine Fisheries Research Institute, Kochi, India, for providing the necessary facilities to carry out this work. The first author also acknowledges the Kerala University of Fisheries and Ocean Studies (KUFOS) for providing a master's degree fellowship.

Conflict of interest

The author(s) declared that this work was conducted in the absence of any commercial or financial relationships that could be construed as a potential conflict of interest.

Generative AI statement

The author(s) declared that generative AI was not used in the creation of this manuscript.

Any alternative text (alt text) provided alongside figures in this article has been generated by Frontiers with the support of artificial intelligence and reasonable efforts have been made to ensure accuracy, including review by the authors wherever possible. If you identify any issues, please contact us.

Publisher's note

Supplementary material

The Supplementary Material for this article can be found online at: https://www.frontiersin.org/articles/10.3389/fmars.2026.1716162/full#supplementary-material

References

Aebi, H. (1984). *Catalase in* vitro. *In* Methods in enzymology Vol. 105 (Academic press), 121–126.

Atli, G., Alptekin, Ö., Tükel, S., and Canli, M. (2006). Response of catalase activity to Ag +, Cd2+, Cr6+, Cu2+ and Zn2+ in five tissues of freshwater fish Oreochromis niloticus. *Comp. Biochem. Physiol. Part C: Toxicol. Pharmacol.* 143, 218–224. doi: 10.1016/j.cbpc.2006.02.003

Atli, G., and Canli, M. (2008). Responses of metallothionein and reduced glutathione in a freshwater fish, *Oreochromis niloticus*, following metal exposures. *Environ. Toxicol. Pharmacol.* 25, 33–38. doi: 10.1016/j.etap.2007.08.007

Bal, A., Panda, F., Pati, S. G., Das, K., Agrawal, P. K., and Paital, B. (2021). Modulation of physiological oxidative stress and antioxidant status by abiotic factors especially salinity in aquatic organisms. *Comp. Biochem. Physiol. Part C: Toxicol. Pharmacol.* 241, 108971. doi: 10.1016/j.cbpc.2020.108971

Bligh, E. G., and Dyer, W. J. (1959). A rapid method of total lipid extraction and purification. *Can. J. Biochem. Physiol.* 37, 911–917. doi: 10.1139/y59-099

Bœuf, G., and Payan, P. (2001). How should salinity influence fish growth? *Comp. Biochem. Physiol. Part C: Toxicol. Pharmacol.* 130, 411–423. doi: 10.1016/S1532-0456(01)00268-X

Chandrasekar, S., Nich, T., Tripathi, G., Sahu, N. P., Pal, A. K., and Dasgupta, S. (2014). Acclimation of brackish water pearl spot (*Etroplus suratensis*) to various salinities: relative changes in abundance of branchial Na+/K+-ATPase and Na+/K+/2Cl– co-transporter in relation to osmoregulatory parameters. *Fish Physiol. Biochem.* 40, 983–996. doi: 10.1007/s10695-013-9899-y

Chen, J., Cai, B., Tian, C., Jiang, D., Shi, H., Huang, Y., et al. (2023). RNA sequencing (RNA-Seq) analysis reveals liver lipid metabolism divergent adaptive response to low- and high-salinity stress in spotted scat (*Scatophagus argus*). *Animals* 13, 1503. doi: 10.3390/ani13091503

Dong, X., Wang, J., Ji, P., Sun, L., Miao, S., Lei, Y., et al. (2020). Seawater culture increases omega-3 long-chain polyunsaturated fatty acids (n-3 LC-PUFA) levels in Japanese sea bass (*Lateolabrax japonicus*), probably by upregulating Elovl5. *Animals* 10, 1681. doi: 10.3390/ani10091681

Drapeau, G. R. (1976). "Protease from *staphyloccus aureus*," in *Methods in enzymology*, vol. 45. (Academic Press), 469–475.

Du, X., Zhang, W., He, J., Zhao, M., Wang, J., Dong, X., et al. (2022). The impact of rearing salinity on flesh texture, taste, and fatty acid composition in largemouth bass *Micropterus salmoides*. *Foods* 11, 3261. doi: 10.3390/foods11203261

Edwards, S. L., and Marshall, W. S. (2012). *Principles and patterns of osmoregulation and euryhalinity in fishes*. (Cambridge, CA: Academic Press) 1–44.

Ern, R., Huong, D. T. T., Cong, N. V., Bayley, M., and Wang, T. (2014). Effect of salinity on oxygen consumption in fishes: a review. *J. Fish Biol.* 84, 1210–1220. doi: 10.1111/jfb.12330

Evans, D. H. (2008). Teleost fish osmoregulation: what have we learned since August Krogh, Homer Smith, and Ancel Keys. *Am. J. Physiology-Regulatory Integr. Comp. Physiol.* 295, R704–R713. doi: 10.1152/ajpregu.90337.2008

Evans, T. G., and Kültz, D. (2020). The cellular stress response in fish exposed to salinity fluctuations. *J. Exp. Zoology Part A: Ecol. Integr. Physiol.* 333, 421–435. doi: 10.1002/jez.2350

Fridman, S. (2020). Ontogeny of the osmoregulatory capacity of teleosts and the role of ionocytes. *Front. Mar. Sci.* 7, 709. doi: 10.3389/fmars.2020.00709

Gora, A. H., Rehman, S., Dias, J., Fernandes, J. M., Olsvik, P. A., Sørensen, M., et al. (2023). Protective mechanisms of a microbial oil against hypercholesterolemia: evidence from a zebrafish model. *Front. Nutr.* 10, 1161119. doi: 10.3389/fnut.2023.1161119

Gora, A. H., Rehman, S., Kiron, V., Dias, J., Fernandes, J. M., Olsvik, P. A., et al. (2022). Management of hypercholesterolemia through dietary ß-glucans–insights from a zebrafish model. *Front. Nutr.* 8, 797452. doi: 10.3389/fnut.2021.797452

Guerrera, M. C., De Pasquale, F., Muglia, U., and Caruso, G. (2015). Digestive enzymatic activity during ontogenetic development in zebrafish (*Danio rerio*). *J. Exp. Zoology Part B: Mol. Dev. Evol.* 324, 699–706. doi: 10.1002/jez.b.22658

Huggett, J., Dheda, K., Bustin, S., and Zumla, A. (2005). Real-time RT-PCR normalisation; strategies and considerations. *Genes Immun.* 6, 279–284. doi: 10.1038/sj.gene.6364190

Imsland, A. K., Foss, A., Gunnarsson, S., Berntssen, M. H., FitzGerald, R., Bonga, S. W., et al. (2001). The interaction of temperature and salinity on growth and food conversion in juvenile turbot (*Scophthalmus maximus*). *Aquaculture* 198, 353–367. doi: 10.1016/S0044-8486(01)00507-5

Jiang, Y., Yuan, C., Qi, M., Liu, Q., and Hu, Z. (2022). The effect of salinity stress on enzyme activities, histology, and transcriptome of silver carp (*Hypophthalmichthys molitrix*). *Biology* 11, 1580. doi: 10.3390/biology11111580

Jin, G., Zhang, L., Ai, Q., Mai, K., and Chen, X. (2025). Interactive effects of salinity and dietary lipid sources on growth, hepatic lipid metabolism, and transcriptomic profiles in spotted sea bass (*Lateolabrax maculatus*). *Front. Physiol.* 16, 1655953. doi: 10.3389/fphys.2025.1655953

Kang, C. K., Tsai, S. C., Lee, T. H., and Hwang, P. P. (2008). Differential expression of branchial Na+/K+-ATPase of two medaka species, *Oryzias latipes* and *Oryzias dancena*, with different salinity tolerances acclimated to fresh water, brackish water, and seawater. *Comp. Biochem. Physiol. Part A: Mol. Integr. Physiol.* 151, 566–575. doi: 10.1016/j.cbpa.2008.07.020

Katsivela, E., Kleppe, F., Lang, S., and Wagner, F. (1995). Ustilago maydis lipase I. Hydrolysis and ester-synthesis activities of crude enzyme preparation. *Enzyme Microbial Technol.* 17, 739–745. doi: 10.1016/0141-0229(94)00127-D

Koper, K., Han, S. W., Pastor, D. C., Yoshikuni, Y., and Maeda, H. A. (2022). Evolutionary origin and functional diversification of aminotransferases. *J. Biol. Chem.* 298, 102122. doi: 10.1016/j.jbc.2022.102122

Kültz, D. (2015). Physiological mechanisms used by fish to cope with salinity stress. *J. Exp. Biol.* 218, 1907–1914. doi: 10.1242/jeb.118695

Li, Y., Han, J., Wu, J., Li, D., Yang, X., Huang, A., et al. (2020). Transcriptome-based evaluation and validation of suitable housekeeping gene for quantification real-time PCR under specific experiment condition in teleost fishes. *Fish shellfish Immunol.* 98, 218–223. doi: 10.1016/j.fsi.2020.01.018

Li, X., Shen, Y., Bao, Y., Wu, Z., Yang, B., Jiao, L., et al. (2022). Physiological responses and adaptive strategies to acute low-salinity environmental stress of the euryhaline marine fish black seabream (*Acanthopagrus schlegelii*). *Aquaculture* 554, 738117. doi: 10.1016/j.aquaculture.2022.738117

Li, Z., Yang, L., Wang, J., Shi, W., Pawar, R. A., Liu, Y., et al. (2010). β-Actin is a useful internal control for tissue-specific gene expression studies using quantitative real-time PCR in the half-smooth tongue sole *Cynoglossus semilaevis* challenged with LPS or *Vibrio Anguillarum*. *Fish shellfish Immunol.* 29, 89–93. doi: 10.1016/j.fsi.2010.02.021

Lin, C. H., Tsai, R. S., and Lee, T. H. (2004). Expression and distribution of Na, K-ATPase in gill and kidney of the spotted green pufferfish, *Tetraodon nigroviridis*, in response to salinity challenge. *Comp. Biochem. Physiol. Part A: Mol. Integr. Physiol.* 138, 287–295. doi: 10.1016/j.cbpb.2004.04.005

Liu, J., Ai, T., Yang, J., Shang, M., Jiang, K., Yin, Y., et al. (2024). Effects of salinity on growth, digestive enzyme activity, and antioxidant capacity of spotbanded scat (*Selenotoca multifasciata*) juveniles. *Fishes* 9, 309. doi: 10.3390/fishes9080309

Liu, Z. F., Gao, X. Q., Yu, J. X., Qian, X. M., Xue, G. P., Zhang, Q. Y., et al. (2017). Effects of different salinities on growth performance, survival, digestive enzyme activity, immune response, and muscle fatty acid composition in juvenile American shad (*Alosa sapidissima*). *Fish Physiol. Biochem.* 43, 761–773. doi: 10.1007/s10695-016-0330-3

Lushchak, V. I. (2011). Environmentally induced oxidative stress in aquatic animals. *Aquat. Toxicol.* 101, 13–30. doi: 10.1016/j.aquatox.2010.10.006

Manirakiza, P., Covaci, A., and Schepens, P. (2001). Comparative study on total lipid determination using Soxhlet, Roese-Gottlieb, Bligh & Dyer, and modified Bligh & Dyer extraction methods. *Journal of Food Composition and Analysis* 14, 93–100. doi: 10.1006/jfca.2000.0972

Marrero, M., Monroig, Ó., Betancor, M., Herrera, M., Pérez, J. A., Garrido, D., et al. (2021). Influence of dietary lipids and environmental salinity on the n-3 long-chain polyunsaturated fatty acids biosynthesis capacity of the marine teleost *Solea* Senegalensis. *Mar. Drugs* 19, 254. doi: 10.3390/md19050254

Martínez-Álvarez, R. M., Morales, A. E., and Sanz, A. (2005). Antioxidant defenses in fish: biotic and abiotic factors. *Rev. Fish Biol. Fish* 15, 75–88. doi: 10.1007/s11160-005-7846-4

Metcalfe, L. D., Schmitz, A. A., and Pelka, J. R. (1966). Rapid preparation of fatty acid esters from lipids for gas chromatographic analysis. *Analytical Chemistry* 38, 514–515. doi: 10.1021/ac60235a044

Metwaly, S., Nasr, H., Ahmed, K., and Fathi, M. (2025). Multifaceted stress response in Nile tilapia (*Oreochromis niloticus*) fingerlings: integrative analysis of salinity, ammonia, and stocking density effects on growth, physiology, and gene expression. *Fish Physiol. Biochem.* 51, 48. doi: 10.1007/s10695-025-01462-6

Misra, H. P., and Fridovich, I. (1977). Superoxide dismutase:"positive" spectrophotometric assays. *Analytical Biochem.* 79, 553–560. doi: 10.1016/0003-2697(77)90429-8

Monroig, Ó., Tocher, D. R., and Navarro, J. C. (2013). Biosynthesis of polyunsaturated fatty acids in marine invertebrates: recent advances in molecular mechanisms. *Mar. Drugs* 11, 3998–4018. doi: 10.3390/md11103998

Morais, S., Pratoomyot, J., Taggart, J. B., Bron, J. E., Guy, D. R., Bell, J. G., et al. (2011). Genotype-specific responses in Atlantic salmon (*Salmo salar*) subject to dietary fish oil replacement by vegetable oil: a liver transcriptomic analysis. *BMC Genomics* 12, 255. doi: 10.1186/1471-2164-12-255

Motamedi-Tehrani, J., Peyghan, R., Shahriari, A., Razijalali, M., and Ebrahimi, E. (2025). The influence of ammonia-N and salinity levels on oxidative stress markers, hepatic enzymes, and acid phosphatase activity in Nile tilapia (*Oreochromis niloticus*). *Sci. Rep.* 15, 559. doi: 10.1038/s41598-024-84136-2

Pfaffl, M. W. (2001). A new mathematical model for relative quantification in real-time RT–PCR. *Nucleic Acids Res.* 29, e45–e45. doi: 10.1093/nar/29.9.e45

Pfaffl, M. W., Tichopad, A., Prgomet, C., and Neuvians, T. P. (2004). Determination of stable housekeeping genes, differentially regulated target genes and sample integrity: BestKeeper–Excel-based tool using pair-wise correlations. *Biotechnol. Lett.* 26, 509–515. doi: 10.1023/B:BILE.0000019559.84305.47

Prieto, P., Pineda, M., and Aguilar, M. (1999). Spectrophotometric quantitation of antioxidant capacity through the formation of a phosphomolybdenum complex: specific application to the determination of vitamin E. *Analytical Biochem.* 269, 337–341. doi: 10.1006/abio.1999.4019

Ramírez-Duarte, W. F., Jin, J., Kurobe, T., and Teh, S. J. (2016). Effects of prolonged exposure to low pH on enzymatic and non-enzymatic antioxidants in Japanese Medaka (*Oryzias latipes*). *Sci. Total Environ.* 568, 26–32. doi: 10.1016/j.scitotenv.2016.05.179

Ramírez-Duarte, W. F., Kurobe, T., and Teh, S. J. (2017). Impairment of antioxidant mechanisms in Japanese Medaka (*Oryzias latipes*) by acute exposure to aluminum. *Comp. Biochem. Physiol. Part C: Toxicol. Pharmacol.* 198, 37–44. doi: 10.1016/j.cbpc.2017.05.003

Ranjan, R., Anil, M. K., Ambarish, G. P., Megarajan, S., Xavier, B., Ghosh, S., et al. (2022). Protocol developed for the hatchery production of marine model fish *Oryzias dancena* (Hamilton 1822). *Mar. Fisheries Inf. Service; Tech. Extension Ser.* 254, 32–35.

Rick, W., and Stegbauer, H. P. (1974). "α-Amylase measurement of reducing groups," in *Methods of enzymatic analysis* (Academic Press), 885–890.

Sargent, J. R., Tocher, D. R., and Bell, J. G. (2003). The lipids. *Fish Nutr.*, 181–257. doi: 10.1016/B978-012319652-1/50005-7

Satkar, S. G., Sudhagar, A., Dharmaratnam, A., Swaminathan, T. R., Sood, N., Abhilash, C. P., et al. (2025). Unravelling the ontogeny and tissue-specific expression profiles of immune-related genes in the near-threatened endemic catfish, Clarias dussumieri. *Fish Shellfish Immunol.* 157, 110075. doi: 10.1016/j.fsi.2024.110075

Schneider, C. A., Rasband, W. S., and Eliceiri, K. W. (2012). NIH Image to ImageJ: 25 years of image analysis. *Nat. Methods* 9, 671–675. doi: 10.1038/nmeth.2089

Sinha, A. K., AbdElgawad, H., Zinta, G., Dasan, A. F., Rasoloniriana, R., Asard, H., et al. (2015). Nutritional status as the key modulator of antioxidant responses induced by high environmental ammonia and salinity stress in European sea bass (*Dicentrarchus labrax*). *PloS One* 10, e0135091. doi: 10.1371/journal.pone.0135091

Si YuFeng, S. Y., Wen HaiShen, W. H., Li Yun, L. Y., He Feng, H. F., Li JiFang, L. J., Li SiPing, L. S., et al. (2018). Liver transcriptome analysis reveals extensive transcriptional plasticity during acclimation to low salinity in *Cynoglossus semilaevis*. *MC Genomics* 19, 464. doi: 10.1186/s12864-018-4825-4

Sutthinon, P., Thongprajukaew, K., Saekhow, S., and Ketmanee, R. (2015). Juvenile hybrid grouper (*Epinephelus coioides*× *E. lanceolatus*) are euryhaline and can grow in a wide range of salinities. *Aquaculture Int.* 23, 671–682. doi: 10.1007/s10499-014-9845-8

Tine, M. (2017). Evidence of the complexity of gene expression analysis in fish wild populations. *Int. J. Genomics* 2017, 1258396. doi: 10.1155/2017/1258396

Tocher, D. R. (2003). Metabolism and functions of lipids and fatty acids in teleost fish. *Rev. fisheries Sci.* 11, 107–184. doi: 10.1080/713610925

Tocher, D. R., Zheng, X., Schlechtriem, C., Hastings, N., Dick, J. R., and Teale, A. J. (2006). Highly unsaturated fatty acid synthesis in marine fish: cloning, functional characterization, and nutritional regulation of fatty acyl Δ6 desaturase of Atlantic cod (Gadus morhua L.). *Lipids* 41, 1003–1016. doi: 10.1007/s11745-006-5051-4

Tocher, D. R. (2010). Fatty acid requirements in ontogeny of marine and freshwater fish. *Aquaculture Res.* 41, 717–732. doi: 10.1111/j.1365-2109.2008.02150.x

Torres-Rodríguez, M., Martínez-Rodríguez, G., Rodríguez-Viera, L., Mancera, J. M., and Martos-Sitcha, J. A. (2025). Physiological effects of water salinity on metabolism and fatty acid biosynthesis in the model fish *fundulus heteroclitus*. *Animals* 15, 2549. doi: 10.3390/ani15172549

Tseng, Y. C., and Hwang, P. P. (2008). Some insights into energy metabolism for osmoregulation in fish. *Comp. Biochem. Physiol. Part C: Toxicol. Pharmacol.* 148, 419–429. doi: 10.1016/j.cbpc.2008.04.009

Varsamos, S., Nebel, C., and Charmantier, G. (2005). Ontogeny of osmoregulation in postembryonic fish: a review. *Comp. Biochem. Physiol. Part A: Mol. Integr. Physiol.* 141, 401–429. doi: 10.1016/j.cbpb.2005.01.013

Woo, N. Y., and Kelly, S. P. (1995). Effects of salinity and nutritional status on growth and metabolism of *Spams sarba* in a closed seawater system. *Aquaculture* 135, 229–238. doi: 10.1016/0044-8486(95)01003-3

Xiao, Y., Zhang, Y. M., Xu, W. B., Chen, D. Y., Li, B. W., Cheng, Y. X., et al. (2022). The effects of salinities stress on histopathological changes, serum biochemical index, non-specific immune and transcriptome analysis in red swamp crayfish *Procambarus clarkii*. *Sci. Total Environ.* 840, 156502. doi: 10.1016/j.scitotenv.2022.156502

Xie, D., Chen, C., Dong, Y., You, C., Wang, S., Monroig, Ó., et al. (2021). Regulation of long-chain polyunsaturated fatty acid biosynthesis in teleost fish. *Prog. Lipid Res.* 82, 101095. doi: 10.1016/j.plipres.2021.101095

Yeh, C. M., Glöck, M., and Ryu, S. (2013). An optimized whole-body cortisol quantification method for assessing stress levels in larval zebrafish. *PloS One* 8, e79406. doi: 10.1371/journal.pone.0079406

Yu, J., Wen, X., You, C., Wang, S., Chen, C., Tocher, D. R., et al. (2021). Comparison of the growth performance and long-chain polyunsaturated fatty acids (LC-PUFA) biosynthetic ability of red tilapia (*Oreochromis mossambicus*♀× *O. niloticus*♂) fed fish oil or vegetable oil diet at different salinities. *Aquaculture* 542, 736899. doi: 10.1016/j.aquaculture.2021.736899

Zhang, N., Yang, R., Fu, Z., Yu, G., and Ma, Z. (2023). Mechanisms of digestive enzyme response to acute salinity stress in juvenile yellowfin tuna (*Thunnus albacares*). *Animals* 13, 3454. doi: 10.3390/ani13223454

Zhou, K., Chen, Z., Qin, J., Huang, Y., Du, X., Zhang, C., et al. (2024). Effects of salinity on muscle nutrition, fatty acid composition, and substance anabolic metabolism of blue tilapia *Oreochromis aureus*. *J. Appl. Ichthyology* 2024, 5549406. doi: 10.1155/2024/5549406